ISSN: 0067-2904

ZnO/CuO/CdS Heterojunction Nanostructures as N-P-N for Optoelectronic Applications Effectiveness of Optoelectronic Devices.

Zehraa Najim Abdul-Ameer
Department of Remote Sensing and GIS, College Science, University of Baghdad, Baghdad, Iraq

Received: 12/6/2022 Accepted: 12/5/2023 Published: 30/5/2024

Abstract

A simple chemical method for producing ZnO/ CuO/ CdS nanoparticles using a chemical route (SILAR) method has been utilized. XRD patterns show hexagonal structures for ZnO, spheres, and cubic-formed CuO/CdS nanoparticles. Nanoparticles showed a blue shift in their UV-VIS energy band edge with (3.7, 3, and 3.2) eV for ZnO, CuO, and CdS. The morphology of ZnO, CuO, and CdS nanoparticles is investigated using scanning electronic microscopy (SEM). The XRD pattern reveals that the crystallites size are 15–30 nm. Photoluminescence reveals a yellow-green (520 nm) region for ZnO, a blue (380 nm) region for CuO, and a red (440 nm) region for CdS. The CdS wideband gap restricts its application. In this manner, we combined ZnO, CdS, and CuO for the band gap design of the heterojunction and to get improved optoelectronic properties. Present results show that heterojunctions could be useful for long-term usage and effective photodiode applications.

Keywords: Heterojunction, nanoparticles, phodiode, ZnO, CuO, CdS.

دراسه تحضير غشاء اوكسيد الزنك/اوكسيد النحاس/كبريتيد الكادميوم غير المتجانس كمفرق n–p–n لتطبيقات الإلكترونية الضوئية وفعالية الأجهزة الإلكترونية الضوئية

زهراء نجم عبد الامير

قسم التحسس النائي، كلية العلوم، جامعة بغداد، بغداد، العراق

الخلاصة

تم استخدام طريقة بسيطة لتحضير الجسيمات النانوية اوكسيد الزنك /اوكسيد النحاس /كبريتيد الكادميوم باستخدام طريقة المسار الكيميائي (SILAR) بالترسيب الطبقي . تُظهر أنماط XRD تركيبا سداسيًا للجسيمات اوكسيد الزنك النانوية ومكعبة لكبريتيد الكادميوم واحادية الميل لاوكسيد النحاس. وأظهرت الجسيمات النانوية ازاحة باتجاه المنطقة الزرقاء في حافة نطاق طاقة UV–VIS مع (3.7 ، 3 ، 3.2) eV لـ اوكسيد الزنك /اوكسيد النحاس /كبريتيد الكادميوم يوضح نمط XRD أن أحجام الجسيمات النانوية هي 15–30 نانومتروبشكل يتفق مع نتائج المجهر الالكتروني الماسح. ظهرت أطياف اللمعان الضوئي لجزيئات CdS النانوية بأقصى ما يقرب من 440 نانومتر بخصائص بصرية وإلكترونية مميزة بسبب مداراتها الإلكترونية غير المملوءة قد قمنا بدمج ZnO و CdS مع Cuo لتصميم فجوة الحزمة للاغشية غير المتجانسة الحصول على

*Email: zehraa.najim@sc.uobaghdad.edu.iq

خصائص إلكترونية ضوئية محسّنة. تظهر النتائج الحالية أن المفارق غير المتجانسة يمكن أن تكون مفيدة للاستخدام على المدى الطويل وتطبيقات الثنائي الضوئي الفعالة.

1. Introduction

Colloidal nanoparticles (NPs) have drawn broad logical and mechanical intrigues due to their size dependant properties, distinctive optical and electrical highlights.These characteristics made colloidal nanoparticles potentially suitable for use in LEDs [1-4]. [5] and photonics devices.

Zinc oxide (ZnO) is an unusually wide bandgap (3.3 eV)semiconductor that exhibits various properties that make it suitable for many mechanical applications, including gas sensors [7], UV and blue light emitters [8], and transistors [9].

Copper (II) oxide (CuO) is another oxide semiconductor that has low bandgap (1.2 eV). It is a P-type semiconductor The bulk CuO has a monoclinic structure. The copper particle is facilitated by 4 oxygen particles in a square planer setup [10,11].

A cadmium sulfide (CdS) photoresistor (or photocell) changes its resistance depending on the light concentration falling on it. It is delicate, quick, and has been around for decades. It is regularly utilized in road lights and as an "electric eye." Note that resistance reduces from millions of ohms in obscurity to as few as many hundred ohms in shining light. A straightforward test is to utilize an ohmmeter and observe the resistance change with light exerted [12]. Cds nanocrystals have prevalent optical and electronic properties due to their unfilled electronic orbitals. In any case, the wideband gap of CdS limits its application.

SILAR method is one of the chemical methods for producing thin films. SILAR's preferences include viability, the ease with which the statement hardware can be made, and the hardware's ability to be made controlled statement rates, and a wide spectrum of statement parameters for the control and optimization of film properties and thickness. SILAR is a chemical deposition method for blending thin films in which the essential building pieces are ions rather than atoms. Therefore, the preparative parameters are effectively controllable.

This study aims to prepare ZnO/CuO/CdS heterojunction nanostructures using the SILAR simple, low-cost method to obtain heterojunction of nanoparticles with properties that can be used in various industrial applications such as fluorescent tube luminous material, active laser media, sensors, and so on.

2. Experimental

2.1 Materials used

1-ZnO Nano rod preparation

Hexamethylenetetramine (HMT) and zinc nitrate (Zn(NO3)2.6H2O) solutions were prepared in a reaction vessel in an equimolar ratio of (0.1M). At that time, the precursor solution (zinc nitrate) was submerging the pre-seeded substrate (ITO)and bake for a few hours at 50 ºC. After the growth of ZnO nanorods, samples were soaked in deionized (DI) water to expel any residuals and then dried. The ZnO NRs thickness, morphological structure, and angle proportion can be controlled by altering the response parameters like precursor concentration, pH value, temperature of growth, and time of growth [12]

2-CuO Nanoparticles:

Copper nitrate (Cu $(NO_3)_2.H_2O$) and HMT were utilized as the precursor solutions(Cu nitrate) for the CuO growth nanoparticles. For the formation of CuO nanoflower structures, (5 mM) copper nitrate and (1 mM) HMT were diluted in deionized water. The substrate was immersed in the reaction vessel, which contained the precursor solution (Cu nitrate). The vessel was stacked in the laboratory oven at 90^{o}C for 4 to 5 hours.

3-CdS nanoparticles preparation:

Thioacetamide (C_2H_5NS) and cadmium nitrate tetrahydrate (Cd $(NO_3)_2.4\ H_2O$) were used as sources of cadmium, with a (1 M) concentration of polyethyleneimine as a surface stabilizer or surfactant for growth control of CdS nanoparticles.

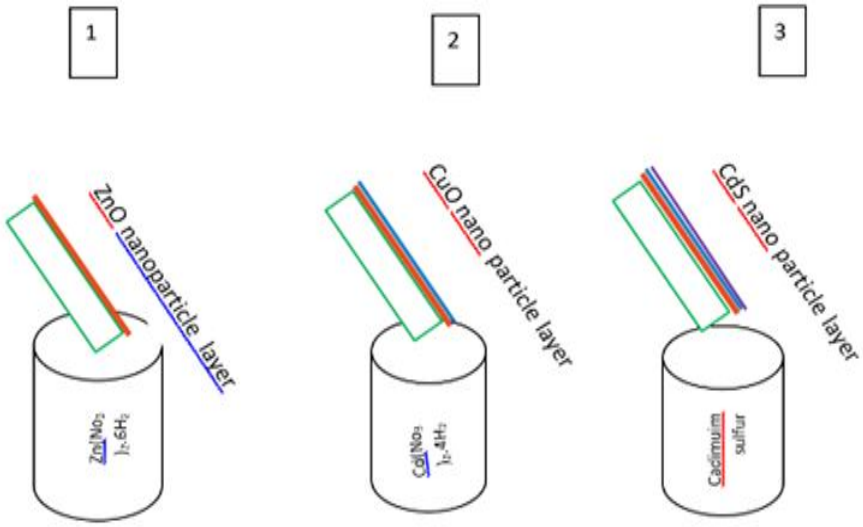

Figure 1: schematic digram of SILAR method

In the SILAR method, the substrate was immersed separately in two precursor solutions and then washed with water to remove loosely bound species. Cation precursor adsorption, water rinsing, anion precursor adsorption, reaction, and yet another rinsing constitute a one SILAR cycle. Figure 1 shows a schematic diagram of the SILAR method.

3. Results and discussion

3.1.X-Ray Diffraction

The crystallite size was calculated using Scherrer's formula, [13]:

$$D= (0.9\ \lambda)/(\beta \cos \theta) \quad \text{…….. [1]}$$

Where: D is the crystallite size, λ is the X-ray wavelength, β is the diffraction line broadening, measured at full width at half maximum (FWHM), and θ is the diffraction angle (deg). The crystallite size and other parameters (broadening, and dislocation density) for ZnO, CuO, CdS [14] are shown in Table (1).

XRD technique was used to study the prepared thin films of ZnO, CuO, CdS, and ZnO /CuO/ CdS heterojunction. Figure 2 shows the XRD patterns of specimens. The lattice parameters of ZnO thin films evaluated from XRD patterns (Figure 2a) are well understood as (JCPDS, 36-1451)[24]. ZnO XRD pattern showed peaks at 100, 002, 101, 102, 110, 103, 200 at **θ**=31.1º, 32.9º, 43.4º, 52.81º, 60.1º, 66.8º, respectively.

All the peaks in the XRD pattern of CuO (Figure2b) can be indexed to the monoclinic structure, as confirmed by the JCPDS, File No. 80-1916. The lattice parameters for CuO show peaks at 020, 021, 110, 002, 111, 042, 130, 131, 151, 113, 200, 152, and 202 corresponding to **θ**=18^{o}, 24.9^{o}, 29.7^{o}, 33.4^{o}, 35.3^{o}, 39.1^{o}, 42.7^{o}, 49.8^{o}, 56.3^{o}, 63.1^{o} ,66.8^{o}, and 74.3^{o}, respectively. The normal crystallite size estimated for CuO nanoparticles calculated from the XRD pattern was 22.3 nm[15].

The XRD pattern of the CdS precipitated NPs are in Figure 2C The peaks are credited to hexagonal CdS (JCPDS – record No. 10-0454). The broad peaks indicate nano size particles. XRD indicates cubic structure. It appeared that the sizes of the nanoparticles between (10-20) nm [16].

Table 1: XRD parameters

parameter	ZnO	CuO	CdS
β (deg)	0.05	0.03	0.087
D (nm)	18.5	22.33	10.4
ε (* 10^{-3})	683	565	1116
δ ($1/nm^2$)	2.9	2	9.2

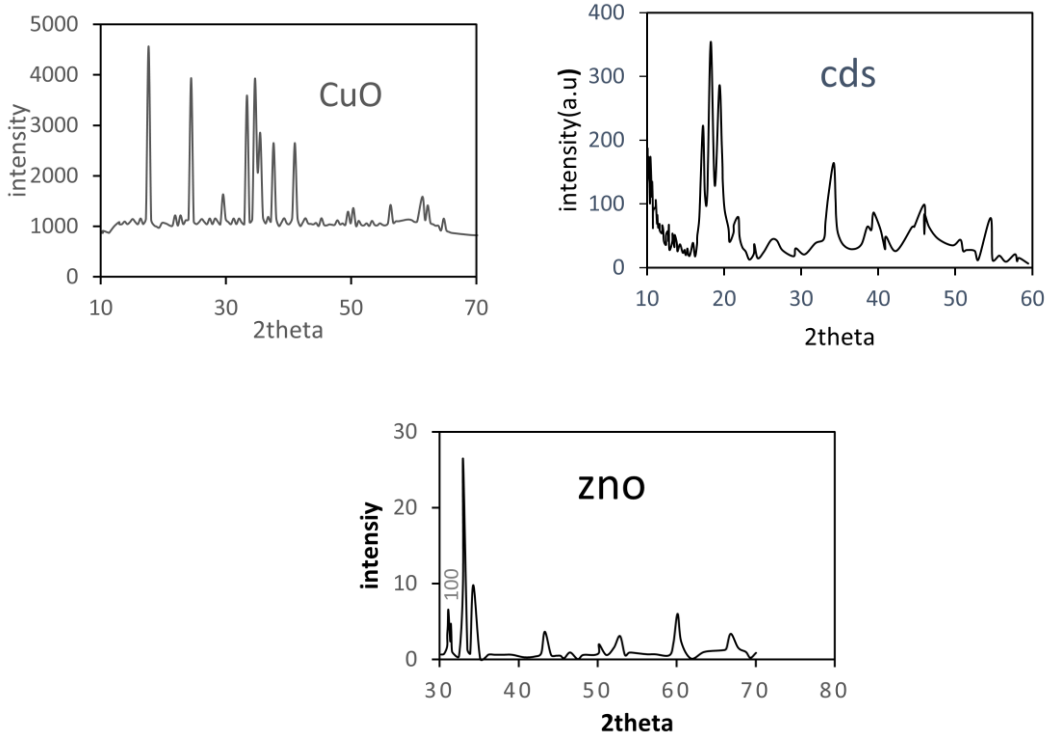

Figure 2: XRD analysis for a-ZnO b-CuO c-CdS

3.2.Optical characteristics

The UV-Visible spectra of CuO nanoparticles are blue-shifted compared to that of the bulk. The energy bandgap (Eg) was calculated from the assimilation spectra.The optical bandgap (Eg) of the thin films was determined using the Tauc plot:

$$(\alpha h\nu)^2=A(h\nu-Eg) \quad \text{.....[3][17]}$$

Energy bandgap was calculated from Fig 2 it was found to be (3eV) due to surface to volume ratio. CuO films have a high thickness of surface, interstitials, and oxygen vacancies. Photoenergy spectroscopy has been utilized to investigate the optical outflow properties of CuO nanoparticles.

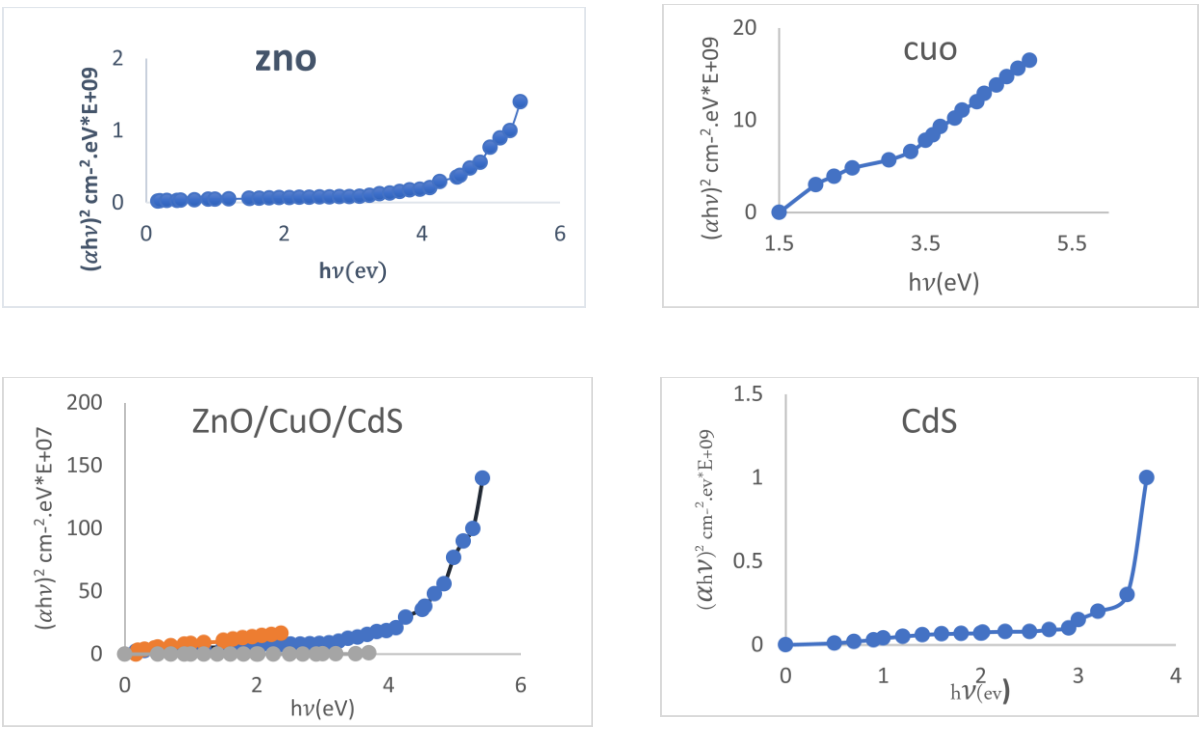

Figure 3: ($\alpha h\nu$ **)**^{2} as a function of h**ν** for ZnO, CuO, CdS, and ZnO/CuO/CdS hetrojunction.

Many photoluminescence bands were generally reported for CuO nanostructures from UV to near IR region. Because of the oxygen vacancy, the most frequent peaks occur between 400 and 600 nm, as opposed to the band edge at 450 nm. The optical properties of the synthesized nanoCdS, as well as UV-Vis estimations, revealed that CdS has a coordinate band and a gap larger than 3.2 eV depending, on the heat treatment and conditions. In this way, heat treatment can be utilized to control nanoparticle size. The emission spectra appeared to be the most extreme at almost 603 nm, with a redshift of approximately 100 nm and an expanding tempering temperature related to the nearness of defect states within the nanoparticles.

Photoluminescence(PL) spetroscopy was used to explore the optical and emission characteristics of CuO nanoparticles. The emission at 420 nm comes from band edge emission, whereas the emission at 600 nm comes from oxygen vacancy emission as in Figure 4.

The crystallite size varies between 15-20 nanometers. Peaks in the yellow-green region (520 nm) may be seen in the PL spectra. The PL low energy suggests that CdS excitonic emission is not the source of PL. Additionally, the excitonic PL band is primarily visible at (440 nm) in the blue region with restricted Cds nanoparticles. Given the levels of deformity compared to the bulk, recombination is most likely the cause[15,16].

Donor-acceptor recombination that includes a state in the CdS band could be the origin of the low energy band. Therefore, the local defects like sulphur, cadmium, and vacancies are

largely responsible for the defect states that contribute to the low energy band edge PL. The low energy band in this study is probably caused by sulphur vacancies[17].

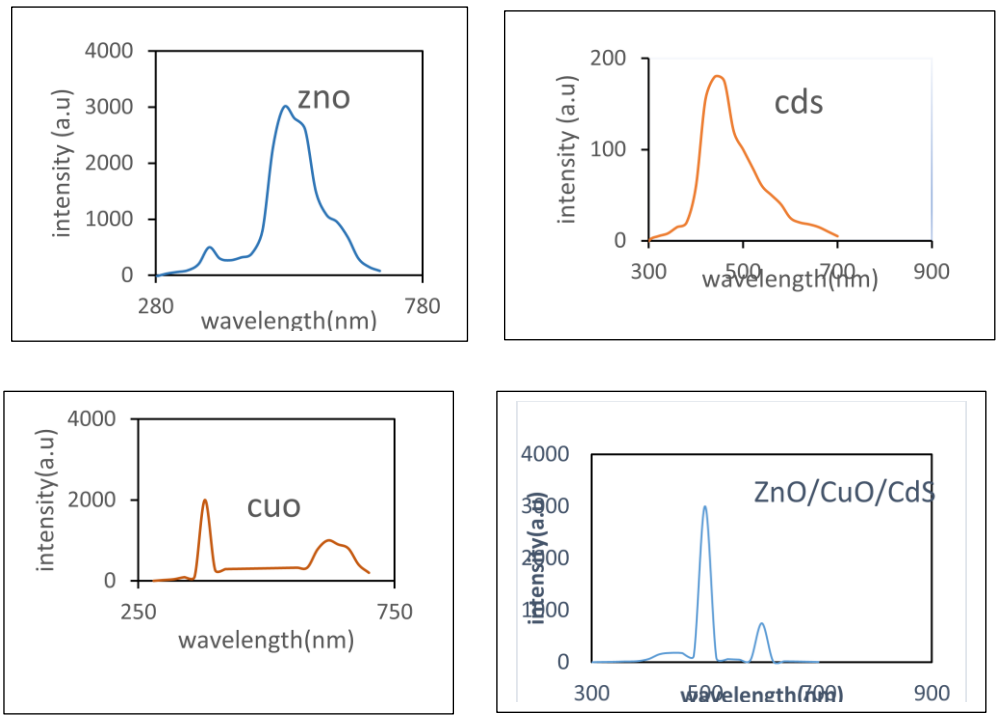

Figure 4: Photoluminescent spectra for ZnO, CuO, CdS,and ZnO/CuO/CdS

3.3 Scanning Electron Microscopy (SEM):

studying the morphology of thin films is an exceptionally important way to explore the microstructure of thin films. Figure 5 shows the surface morphological structure of the synthesized films. SEM images clearly shows the stoichiometric formation of ZnO nano-crystals of rod-shape. ZnO nanorods have uniform shape and length, align vertically on the substrate.CuO images show the formation of nano branches with nanoclusters here and there. The formation of some dislocations and vacancies could be noticed. While CdS images show uniform nano spheres and less vacancies in comparison with ZnO and CuO. The heterostructure images of ZnO/CuO/CdS have more horizontal branches with existence of nanospheres that appear in small clusters.

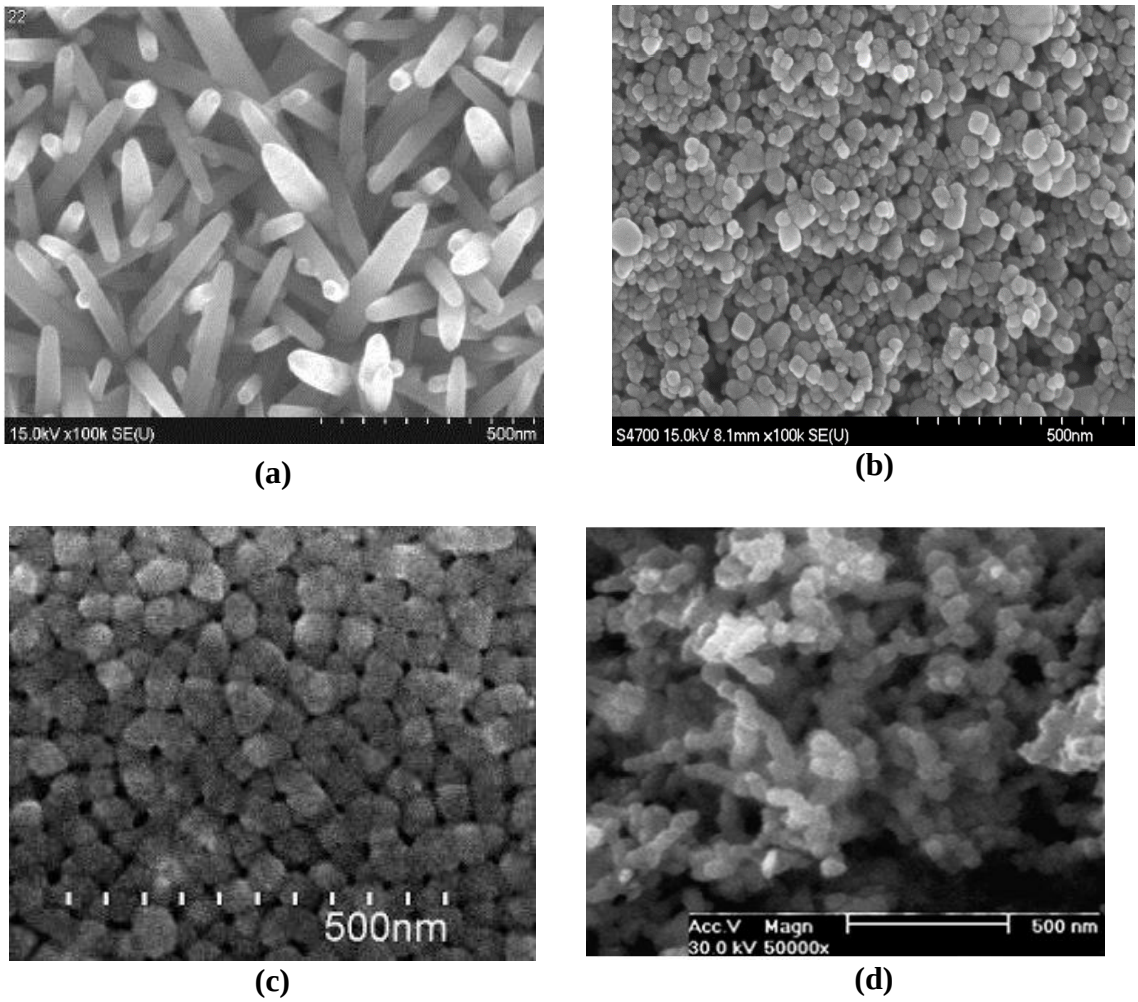

Figure 5: SEM for a -ZnO b-CuO C-CdS d-ZnO/CuO/CdS Hetereojunction

3.4 Current-Voltage Characteristics:

Current-voltage characteristics curves (IV curves) of an electrical component shows the relation between the current passing through it and the voltage applied across it. It is a family of curves that shows the operation of a certain electronic component in an electrical circuit.

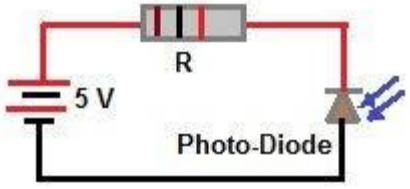

Figure 6: A photodiode circuit.

Figure(6) shows a photodiode connected in an electrical circuit to study its IV characteristic curves. The diode is biased by the 5V battery in order to be used as a practical device or as a rectifying device. By the same manner the heterojunction ZnO/CuO/CdS was connected in an electrical circuit and its IV characteristic curve is as shown in Figure 7.

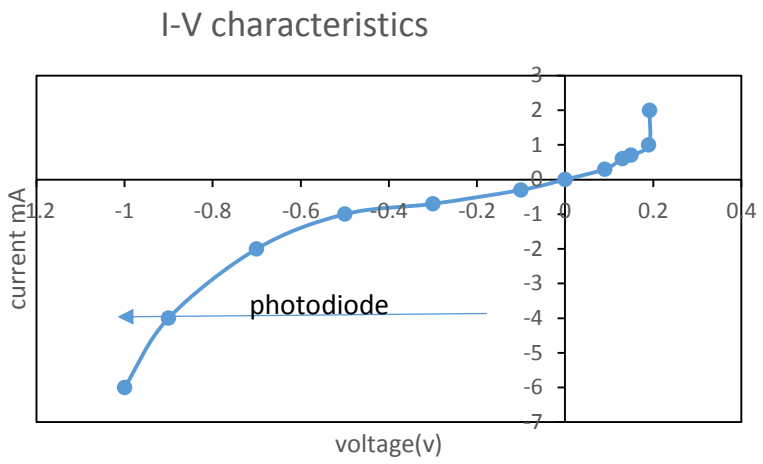

Figure 7: IVcharacteristics for heterojunction ZnO/CuO/CdS

The current-voltage characteristics vary in light as in Figure 7. The reverse current rises as a result of the photocurrent generation[20]. The IV characteristics of the ZnO/CuO/CdS heterojunction device when forward biased indicates the possibility of solar manner, which represents IV characteristics under illumination; while with reverse biasing it shows the I-V characteristics in the dark. However, the curve shows good behavior as a photodiode [21,22].

4. Conclusions

A study of heterojunction of nano ZnO/CuO/CdS particles prepared by a simple method using a chemical route (SILAR) method was presented. XRD patterns show hexagonal structure for ZnO and CdS, and monoclinic for CuO. Nanoparticles showed blue shift in their UV-VIS energy band edge with (3.7, 3, 3.2) eV for ZnO, CuO, and CdS. SEM is used to study the structure, morphology of ZnO,CuO,CdS individually, Photoluminescence reveals a yellow-green (520 nm) region for ZnO, a blue (380 nm) region for CuO, and a red (440 nm) region for CdS. CdS wide band gap restricts its application to this unmistakable local. In this manner, we combined ZnO, CdS, and CuO for the band gap design of the heterojunction and to get improved optoelectronic properties. Present results show that heterojunctions could be useful for long-term usage and effective photodiode applications.

3.6. Acknowledgements

Ministry of sciences and technology/Baghdad/Iraq

References

[1] X. Peng et al., "Shape control of CdSe nanocrystals," *Nature*, vol. 404, pp. 59–61, 2000, doi: 10.1038/35003535

[2] W. U. Huynh, J. J. Dittmer, and A. P. Alivisatos, "Hybrid Nanorod-Polymer Solar Cells," *Science*, vol. 295, no. 5564, pp. 2425–2427, 2002, doi: 10.1126/science.1069156.

[3] R. B. Solanki and P. Rajaram, "Structural, optical and morphological properties of CdS nanoparticles synthesized using hydrazine hydrate as a complexing agent," *Nano-Structures and Nano-Objects*, vol. 12, pp. 157–165, 2017, doi:10.1016/j.nanoso.2017.10.003

[4] Y. Li, A. Rizzo, R. Cingolani, and G. Gigli, "Bright White-Light-Emitting Device from Ternary Nanocrystal Composites," *Advanced Materials*, vol. 18, no. 19, pp. 2545–2548, 2006, doi: 10.1002/adma.200600181.

[5] Y.-W. Lin, W.-L. Tseng, and H.-T. Chang, "Using a Layer-by-Layer Assembly Technique to Fabricate Multicolored-Light-Emitting Films of CdSe@CdS and CdTe Quantum Dots," *Advanced Materials*, vol.18, no. 11, pp. 1381-1386, 2006.

doi.org/10.1002/adma.200502515

[6] F. Fleischhaker and R. Zentel, "Photonic Crystals from Core-Shell Colloids with Incorporated Highly Fluorescent Quantum Dots," *Chemistry of Materials*, vol. 17, no. 6, pp. 1346–1351, Feb. 2005, doi: 10.1021/cm0481022.

[7] Z. Najim and I. Agool, "Synthesis of ZnO-CdO Nanocomposite using Spray Pyrolysis Method and it's Effect on Structural and Optical Properties," *Advances in Natural and Applied Sciences*, vol. 10, no. 1, pp. 1995-0772, 2016, http://www.aensiweb.com/ANAS

[8] J. K. Jaiswal and S. M. Simon, "Potentials and pitfalls of fluorescent quantum dots for biological imaging," *Trends in Cell Biology*, vol. 14, no. 9, pp. 497–504, 2004, doi: 10.1016/j.tcb.2004.07.012

[9] Yue *et al.*, "Facile fabrication of MgZnO/ZnO composites for high performance thin film transistor,"*Journal of Alloys and Compounds*, vol. 873, p. 159840, 2021, doi: 10.1016/j.jallcom.2021.159840.

[10] Z.N.Abdul-Ameer, "Simple Low-Cost Cupric Oxide Nanoparticle Synthesis Using Co-Precipitation Method as a Photodetector Application," *Advances in Environmental Biology*, vol. 10 , no. 6, pp. 60-65, 2016. http://www.aensiweb.com/AEB/

[11] G. Filipič and U. Cvelbar, "Copper oxide nanowires: a review of growth," *Nanotechnology*, vol. 23, no. 19, p. 194001, 2012. doi: 10.1088/0957-4484/23/19/194001.

[12] I. H. Hadi, K. S. Khashan, and D. Sulaiman, "Cadmium sulphide (CdS) nanoparticles: Preparation and characterization," *Materials Today: Proceedings*, vol. 42, no. 5, pp. 3054–3056, 2021, doi: 10.1016/j.matpr.2020.12.828.

[13] E. D. T. Atkins, "Elements of X-ray Diffraction," *Physics Bulletin*, vol. 29, no. 12, p. 572, Dec. 1978, doi: 10.1088/0031-9112/29/12/034.

[14] Z.N.Abdul-Ameer and I. R. Agool, "Structural and Optical Properties of ZnO-CdO Nanocomposite Using Electrodeposition Method," *International Letters of Chemistry*, Physics and Astronomy, vol. 63, pp. 127–133,. 2016, doi: 10.18052/www.scipress.com/ilcpa.63.127.

[15] E.C.Terrazas et.al., "A simple method for the synthesis of CdS Nanopaeclesusing Anonel sufactant," *Chalcogenide Letters*, vol. 12, no. 4, 2015, https://www.researchgate.net /publication /274638845_A_simple_method_for_the_synthesis_of_CdS_nanoparticles_using_a_novel_surfactant

[16] R. S. Mishra, R. Jayakrishnan, and P. Ayyub, "Effect of the size-induced structural transformation on the band gap in CdS nanoparticles," *Journal of Physics: Condensed Matter*, vol. 12, no. 50, pp. 10647–10654, 2000, doi: 10.1088/0953-8984/12/50/325.

[17] J. Yang, F. C. Meldrum, and J. H. Fendler, "Epitaxial Growth of Size-Quantized Cadmium Sulfide Crystals Under Arachidic Acid Monolayers," *The Journal of Physical Chemistry*, vol. 99, no. 15, pp. 5500–5504, 1995, doi: 10.1021/j100015a037.

[18] H. Yang, S. J. Chua, B. X. Liu, L. M. Gan, C.-H. Chew, and G. F. Xu, "Luminescence characteristics of impurities-activated ZnS nanocrystals prepared in microemulsion with hydrothermal treatment," *Applied Physics Letters*, vol. 73, no. 4, pp. 478–480, 1998, doi: 10.1063/1.121906.

[19] M. Bashahu and P. Nkundabakura, "Review and tests of methods for the determination of the solar cell junction ideality factors," *Solar Energy*, vol. 81, no. 7, pp. 856–863, 2007, doi: 10.1016/j.solener.2006.11.002.

[20] B.Anderson, R. Anderson, "Fundamentals of semiconductor devices", Anderson McGraw-Hill, 2016.

[21] A. S. Mohammed, I. M. Ibrahim, and A. Ramizy, "Energy Band Diagram of NiO: Lu2 O3/n-Si heterojunction", Iraqi Journal of Science, vol. 59, no. 1B, pp. 287–293, 2018.

[22] H. A. Hameed, J. J. Hassan, and H. L. Saadon, "Fabrication and Enhancement UV Photodiode Based on Mg-Doped ZnO Nanorods Films", *Iraqi Journal of Science*, Special Issue, The Fourth Conference for Low Dimensional Materials and it's Applications, pp. 7-16, 2018